The current issue and full text archive of this journal is available at
www.emeraldinsight.com/0961-5539.htm

Received 9 October 2006
Revised 28 February 2007
Accepted 6 March 2007

The unsteady boundary layer flow past a circular cylinder in micropolar fluids

Anati Ali and Norsarahaida Amin
Department of Mathematics, Faculty of Science, Universiti Teknologi Malaysia, Johor, Malaysia, and
Ioan Pop
Faculty of Mathematics, University of Cluj, Cluj, Romania

Abstract

Purpose – The purpose of this paper is to study the unsteady boundary layer flow of a micropolar fluid past a circular cylinder which is started impulsively from rest.

Design/methodology/approach – The nonlinear partial differential equations consisting of three independent variables are solved numerically using the 3D Keller-box method.

Findings – Numerical solutions for the velocity profiles, wall skin friction and microrotation profiles are obtained and presented for various values of time t and material parameter K with the boundary condition for microrotation $n = 0$ (strong concentration of microelements) and $n = 1/2$ (weak concentration of microelements). The results are presented along the points on the cylinder surface, starting from the forward to the rear stagnation point, for small time up to the time when the boundary layer flow separates from the cylinder.

Originality/value – It is believed that this is the first paper that uses the 3D Keller-box method to study the unsteady boundary layer flow of micropolar fluids. In the last four decades, there has been overhelming interest shown by researchers in micropolar fluids and still many problems are unsolved. The paper shows not only the fundamental importance of this problem, but also the implications for situations of practical interest.

Keywords Boundary layers, Fluid phenomena, Turbulent flow

Paper type Research paper

Nomenclature

a = radius of the cylinder
C_f = skin friction coefficient
j = microinertia density
K = material parameter
n = ratio of the microrotation vector component and the fluid skin friction at the wall
N = non-dimensional component of the microrotation vector normal to x-y plane
Re = Reynolds number
t = non-dimensional time
u, v = non-dimensional velocity components along x- and y-axes
$u_e(x)$ = non-dimensional external velocity
U_∞ = reference velocity
x, y = non-dimensional Cartesian coordinates along the surface of the cylinder and normal to it, respectively

The first author would like to thank the Public Services Department of Malaysia and Universiti Teknologi Malaysia for financial support. The authors wish also to express their very sincere thanks to the reviewers for their interesting and valuable comments.

International Journal of Numerical Methods for Heat & Fluid Flow
Vol. 17 No. 7, 2007
pp. 692-714

0961-5539
DOI 10.1108/09615530710777967

Greek symbols

γ = spin gradient viscosity
η = semi-similarity variable
κ = vortex viscosity
μ = dynamic viscosity
ν = kinematic viscosity
ρ = density
$\bar{\tau}_w$ = wall skin friction
ψ = non-dimensional stream function at the plate

Subscripts

w = wall condition
∞ = far field condition

Introduction

Unsteady flows have become important in recent years as both a distinct category of fluid mechanics and an area of convective heat and mass transfer. Studies of such flows have been carried out for numerous geometries and under various boundary conditions and fluid properties. Historically these analyses were performed on a boundary-layer basis and mostly addressed applications involving external transport of a steady-state nature. However, some problem areas which are uniquely of a classical boundary-layer nature and which are important in applications, as well as in theory, still persist. An important feature of these flows is that they can be self-similar, sometimes they are non-similar and sometimes they are even of a non-boundary-layer type. Clearly, the introduction of time in the unsteady problem as the extra independent variable increases the complexity of the solution procedure. It is worth mentioning to this end that unsteady forced convection viscous flows were first studied by Stokes (1851) and Rayleigh (1911) and this was long before Prandtl (1905) laid the foundation of the boundary-layer theory. The unsteady nature of a wide range of fluid flows of practical importance has received considerable new attention in recent years. Comprehensive literature reviews on unsteady boundary layers can be found in the review papers by Riley (1975, 1990), Tani (1977), McCroskey (1977) and Telionis (1979), and in the book by Telionis (1981).

Studies of micropolar fluids have recently received considerable attention due to their application in a number of processes that occur in industry. Such applications include: extrusion of polymer fluids, solidification of liquid crystals, cooling of a metallic plate in a bath, animal bloods, exotic lubricants and colloidal and suspension solutions, for example, for which the classical Navier-Stokes theory is inadequate. In this theory, rigid particles contained in a small fluid volume element are limited to rotation about the center of the volume element described by the micro-rotation vector. Here, the laws of classical continuum mechanics are augmented with additional equations that account for the conservation of micro-inertia moments and the balance of first stress moments that arise due to consideration of the microstructure in a material, and also additional local constitutive parameters are introduced. Physically, micropolar fluids may be described as the non-Newtonian fluids consisting of dumb-bell molecules or short rigid cylindrical elements, polymer fluids, fluid suspensions, animal blood, etc. The presence of dust or smoke, particularly in a gas, may also be modeled using micropolar fluid dynamics.

The theory of micropolar fluids, has been first proposed by Eringen (1966, 1972). The key points to note in the development of Eringen's microcontinuum mechanics are the introduction of new kinematic variables, e.g. the gyration tensor and microinertia moment tensor. However, a serious difficulty is encountered when this theory is applied to real, nontrivial flow problems; even for the linear theory, a problem dealing with simple micro fluids must be formulated in terms of a system of 19 partial differential equations in nineteen unknowns and the underlying mathematical problem is not easily amenable to solution. These special features for micropolar fluids were discussed in two

comprehensive review paper of the subject and application of micropolar fluid mechanics by Ariman *et al.* (1973, 1974) and in the books by Łukaszewicz (1999) and Eringen (2001).

The classical problem of unsteady boundary layer flow of a viscous and incompressible fluid past a circular cylinder has been considered by many authors, such as, Wang (1967, 1968), Collins and Dennis (1973a, b), Bar-Lev and Yang (1975), Katagiri (1976), Patel (1976), Cebeci (1979, 1986), Ingham (1984) and Nam (1990). Cebeci (1979) used the two-point Keller-box with zigzag differencing in dealing with the flow reversal. The two-point Keller-box with characteristic box scheme was used by Cebeci (1986). In both of these papers by Cebeci (1979, 1986), the two-point Keller-box differencing scheme which we call the 3D Keller box scheme was used for the problem without flow reversal. The generalized differential quadrature in combination with the generalized integral quadrature (GDQ-GIQ) approach has been used by Shu *et al.* (1996) to study the unsteady boundary layer flows past an impulsively started circular cylinder and it was shown that the numerical instability breaks down the calculation at $t = 3.0$. From the numerical results, they concluded that there is a finite time singularity in the solution of the unsteady boundary layer equation.

In micropolar fluids, the research on steady boundary layer flow past a cylinder has received considerable attention. Nath (1976) considered the steady problem around a cylinder and a sphere in micropolar fluids. The solutions were obtained using an implicit finite difference. He found that in micropolar fluid, the separation occurs at earlier streamwise location as compared to Newtonian fluids. The microrotation parameter does not give much effect to the skin friction and velocity profiles but it gives effect to the microrotation profiles and microrotation gradient. Hassanien *et al.* (1996) considered a steady boundary layer flow at an axisymmetric stagnation point on infinite circular cylinder. They developed a numerical procedure based on Chebyshev polynomials and found that micropolar fluids display a reduction in drag compared to those for Newtonian fluid. The wall shear and couple stresses increases with the increasing values of the material parameter.

The unsteady boundary layer flow of a micropolar fluid near the forward and rear stagnation point of a cylindrical surface which is impulsively started from rest was studied by Lok *et al.* (2003c). They considered the problem for both near the forward and rear stagnation point. Their numerical results for the transient solution were obtained by implementing the 2D Keller-box method. They found that the skin friction coefficient increases as the values of the material parameter K increase. Near the forward stagnation point, the velocity and microrotation profiles attain the steady flow case as time progresses. Near the rear stagnation point, the separation occurs at the same value of time t for any value of K when the parameter n takes the value $n = 1/2$. In a next paper, Lok *et al.* (2003a) have studied the problem of steady two-dimensional asymmetric stagnation point flow of a micropolar fluid. More recently, Kamal and Siddiqui (2004) studied the unsteady flow around a rotating and oscillating circular cylinder in a micropolar fluid. It was found that when there is no rotation of circular cylinder, the separation in the spin was observed but this separation dissolves when the rotation is imposed.

The aim of this paper is to study the problem of unsteady boundary layer flow past a circular cylinder placed in a micropolar fluid by using the implicit 3D Keller-box method as described by Cebeci (1979, 1986). The flow is driven by the impulsive motion of the cylinder from rest. Numerical results are presented for the transient (small time) solution up to the separation point along the cylinder surface including the

stagnation point. The formulation of the problem is discussed in second section. Numerical solutions in the form of velocity profiles, microrotation profiles, wall shear stress and skin frictions are discussed in the third section. To our best knowledge, this problem has not been studied before and it would be of great value to applied mathematicians and engineers working in the area of micropolar fluids. During recent years, the subject on unsteady boundary layer flow of micropolar fluids has received a considerable stimulus and, we have also quoted here some of the classical review papers on the unsteady boundary layer flow of viscous and incompressible fluids (Newtonian fluids).

Problem formulation

We consider the unsteady two-dimensional boundary layer flow of a viscous and incompressible micropolar fluid past a circular cylinder of radius a, which at time $\bar{t} = 0$ is started impulsively from rest with the velocity $\bar{u}_e(\bar{x})$ of the inviscid (potential) fluid, the flow being perpendicular to the axis of the cylinder. This problem is modeled in a rectangular Cartesian coordinate $(\bar{x}, \bar{y})$, where $\bar{x}$ is the coordinate measured along the surface of the cylinder started from its forward stagnation point ($\bar{x} = 0$) and $\bar{y}$ is the coordinate measured in the normal direction to the wall, respectively. The boundary layer equations governing the unsteady boundary layer flow of micropolar fluid are:

$$\frac{\partial \bar{u}}{\partial \bar{x}} + \frac{\partial \bar{v}}{\partial \bar{y}} = 0 \tag{1}$$

$$\frac{\partial \bar{u}}{\partial \bar{t}} + \bar{u}\frac{\partial \bar{u}}{\partial \bar{x}} + \bar{v}\frac{\partial \bar{u}}{\partial \bar{y}} = \bar{u}_e\frac{d\bar{u}_e}{d\bar{x}} + \left(\frac{\mu + \kappa}{\rho}\right)\frac{\partial^2 \bar{u}}{\partial \bar{y}^2} + \frac{\kappa}{\rho}\frac{\partial \bar{N}}{\partial \bar{y}} \tag{2}$$

$$\rho j\left(\frac{\partial \bar{N}}{\partial \bar{t}} + \bar{u}\frac{\partial \bar{N}}{\partial \bar{x}} + \bar{v}\frac{\partial \bar{N}}{\partial \bar{y}}\right) = \gamma\frac{\partial^2 \bar{N}}{\partial \bar{y}^2} - \kappa\left(2\bar{N} + \frac{\partial \bar{u}}{\partial \bar{y}}\right) \tag{3}$$

where $\bar{u}$ and $\bar{v}$ are the velocity component in the $\bar{x}$ and $\bar{y}$ directions, $\bar{N}$ is the component of the microrotation vector normal to the $\bar{x} - \bar{y}$ plane, ρ is the density, κ is the vortex viscosity, γ is the spin-gradient viscosity and j is the microinertia density. Equations (1)-(3) are subject to the initial and boundary conditions:

$$\begin{gathered} \bar{t} < 0 : \bar{u} = \bar{v} = \bar{N} = 0 \quad \text{for any } x, y \\ \bar{t} \geq 0 : \bar{u} = \bar{v} = 0, \quad \bar{N} = -n\frac{\partial \bar{u}}{\partial \bar{y}} \quad \text{at} \quad \bar{y} = 0 \\ \bar{u} = \bar{u}_e(\bar{x}), \quad \bar{N} = 0 \quad \text{as} \quad \bar{y} \to \infty \end{gathered} \tag{4}$$

where n is a constant such that $0 \leq n \leq 1$. It should be mentioned that the case $n = 0$, called strong concentration by Guram and Smith (1980), indicating $N = 0$ near the wall, represents concentrated particle flows in which the microelements close to the wall surface are unable to rotate (Jena and Mathur, 1981). The case $n = 1/2$ indicates the vanishing of anti-symmetrical part of the stress tensor and denotes weak concentration (Ahmadi, 1976). The case $n = 1$ is used for the modeling of turbulent boundary layer flows.

We introduce now the following non-dimensional variables:

$$\begin{gathered} x = \bar{x}/a, \quad y = Re^{1/2}(\bar{y}/a), \quad t = (U_\infty/a)\bar{t}, \quad u = \bar{u}/U_\infty \\ v = Re^{1/2}(\bar{v}/U_\infty), \quad N = (a/U_\infty)Re^{-1/2}\bar{N}, \quad u_e(x) = \bar{u}_e(\bar{x})/U_\infty \end{gathered} \tag{5}$$

where $Re = U_\infty a/\upsilon$ is the Reynolds number and υ is the kinematic viscosity of the fluid. We assume that the spin-gradient viscosity γ has the form:

$$\gamma = (\mu + \kappa/2)j \tag{6}$$

which is invoked to allow the field equations of micropolar fluids predict the correct behavior in the limiting case when microstructure effects become negligible and the total spin $\bar{N}$ reduces to the angular velocity. The derivation of equation (6) has been given by Ahmadi (1976) and Kline (1977). It has been used by many authors in their papers on micropolar boundary layer flow problems, such as Gorla (1988), Yücel (1989), Rees and Bassom (1996), etc. Substituting equation (5) into equations (1)-(3) and using equation (6), we obtain the following non-dimensional form of these equations:

$$\frac{\partial u}{\partial x} + \frac{\partial v}{\partial y} = 0 \tag{7}$$

$$\frac{\partial u}{\partial t} + u\frac{\partial u}{\partial x} + v\frac{\partial u}{\partial y} = u_e\frac{\mathrm{d}u_e}{\mathrm{d}x} + (1+K)\frac{\partial^2 u}{\partial y^2} + K\frac{\partial N}{\partial y} \tag{8}$$

$$\frac{\partial N}{\partial t} + u\frac{\partial N}{\partial x} + v\frac{\partial N}{\partial y} = (1+K/2)\frac{\partial^2 N}{\partial y^2} - K\left(2N + \frac{\partial u}{\partial y}\right) \tag{9}$$

where $K = \kappa/\mu$ is the micropolar (material) parameter and we have taken $j = a\upsilon/u_\infty$. The initial and boundary condition (4) also become:

$$\begin{gathered} t < 0 : u = v = N = 0 \quad \text{for any } x, y \\ t \geq 0 : u = v = 0, \quad N = -n\tfrac{\partial u}{\partial y} \quad \text{at } y = 0 \\ u = u_e(x), \quad N = 0 \quad \text{as } y \to \infty \end{gathered} \tag{10}$$

We introduce now the following non-similarity variables:

$$\psi = t^{1/2}u_e(x)f(x,\eta,t), \quad N = t^{-1/2}u_e(x)g(x,\eta,t), \quad \eta = y/t^{1/2} \tag{11}$$

where ψ is the stream function defined as $u = \partial\psi/\partial y$ and $v = -\partial\psi/\partial x$. Using equations (11), (8) and (9) can be written as:

$$(1+K)f''' + \frac{\eta}{2}f'' + t\frac{\mathrm{d}u_e}{\mathrm{d}x}[1 - (f')^2 + ff''] + Kg' = t\left[\frac{\partial f'}{\partial t} + u_e\left(f'\frac{\partial f'}{\partial x} - f''\frac{\partial f}{\partial x}\right)\right] \tag{12}$$

$$\left(1+\frac{K}{2}\right)g + \frac{\eta}{2}g' + \frac{1}{2}g + t\frac{\mathrm{d}u_e}{\mathrm{d}x}(fg' - f'g) = t\left[\frac{\partial g}{\partial t} + u_e\left(f'\frac{\partial g}{\partial x} - g'\frac{\partial f}{\partial x}\right) + K(2g + f'')\right] \tag{13}$$

subject to the boundary conditions:

$$\begin{gathered} f = f' = 0, \quad g = -nf'' \quad \text{at } \eta = 0 \\ f' = 1, \quad g = 0 \quad \text{at } \eta = \eta_\infty \end{gathered} \tag{14}$$

where η_∞ denotes the value of η at the edge of the boundary layer and primes denote partial differentiation with respect to η.

Following Cebeci (1979), we assume in this paper that $u_e(x)$ has the form:

$$u_e(x) = \frac{1}{\pi}\sin(\pi x) \tag{15}$$

Thus, at the forward stagnation point ($x = 0$), $u_e(x)$ and du_e/dx so that equations (12) and (13) reduce to:

$$(1+K)f''' + \frac{\eta}{2}f'' + Kg'' + t[1-(f')^2 + ff''] = t\frac{\partial f'}{\partial t} \tag{16}$$

$$(1+K/2)g'' + \frac{\eta}{2}g' + \frac{1}{2}g + t(fg'' - f'g) = t\left[\frac{\partial g}{\partial t} + K(2g + f'')\right] \tag{17}$$

On the other hand, at the rear stagnation point ($x = 1$), $u_e(x)$ and $du_e/dx = -1$. Equations (12) and (13) reduces now to:

$$(1+K)f''' + \frac{\eta}{2}f'' + Kg'' - t[1-(f')^2 + ff''] = t\frac{\partial f'}{\partial t} \tag{18}$$

$$(1+K/2)g'' + \frac{\eta}{2}g' + \frac{1}{2}g - t(fg'' - f'g) = t\left[\frac{\partial g}{\partial t} + K(2g + f'')\right] \tag{19}$$

In general, equations (16)-(19) can be written as:

$$(1+K)f''' + \frac{\eta}{2}f'' + Kg'' + t\lambda[1-(f')^2 + ff''] = t\frac{\partial f'}{\partial t} \tag{20}$$

$$(1+K/2)g'' + \frac{\eta}{2}g' + \frac{1}{2}g + t\lambda(fg'' - f'g) = t\left[\frac{\partial g}{\partial t} + K(2g + f'')\right] \tag{21}$$

where $\lambda = 1$ for $x = 0$ and $\lambda = -1$ for $x = 1$. The boundary conditions of equations (20) and (21) are given by equation (14).

For the case $n = 1/2$, we may take:

$$g = -\frac{1}{2}f'' \tag{22}$$

and equations (12) and (13) reduce to:

$$(1+K/2)f''' + \frac{\eta}{2}f'' + t\frac{du_e}{dx}(1 - f'^2 + ff'') = t\left[\frac{\partial f'}{\partial t} + u_e\left(f'\frac{\partial f'}{\partial x} - f''\frac{\partial f}{\partial x}\right)\right] \tag{23}$$

subject to the boundary conditions:

$$f = f' = 0 \quad \text{at } \eta = 0; \quad f' = 1 \quad \text{as } \eta \to \infty \tag{24}$$

If we take:

$$\hat{f}(x, \hat{\eta}, t) = (1+K/2)^{-1/2} f(x, \eta, t), \quad \hat{\eta} = (1+K/2)^{-1/2}\eta \tag{25}$$

Equation (23) reduces to:

$$\hat{f}''' + \frac{\hat{\eta}}{2}\hat{f}'' + t\frac{du_e}{dx}(1 - \hat{f}'^2 + \hat{f}\hat{f}'') = t\left[\frac{\partial \hat{f}'}{\partial t} + u_e\left(\hat{f}'\frac{\partial \hat{f}'}{\partial x} - \hat{f}''\frac{\partial \hat{f}}{\partial x}\right)\right] \tag{26}$$

and the boundary condition (24) becomes:

$$\hat{f} = \hat{f}' = 0 \quad \text{at } \hat{\eta} = 0; \quad \hat{f}' = 1 \quad \text{as } \hat{\eta} \to \infty \tag{27}$$

It should be noticed that equations (26) and (27) are identical with equations (7) and (8) from the paper by Cebeci (1979) for the unsteady boundary layer flow of a viscous and incompressible (Newtonian) fluid past a circular cylinder which is started impulsively from rest. The solution of equation (26) subjected to equation (27) at the initial time $t = 0$ is given by equation (13) in the paper by Cebeci (1979). Thus, the solution of equation (23) subjected to equation (24) at the initial time $t = 0$ can be expressed as:

$$\begin{aligned} f''(\eta) &= \left(\tfrac{1+K/2}{\pi}\right)^{1/2} \exp\left[-\tfrac{\eta^2}{4}(1+K/2)\right] \\ f'(\eta) &= \operatorname{erf}\left[\tfrac{\eta}{2}(1+K/2)^{1/2}\right] \\ f(\eta) &= \eta \operatorname{erf}\left[\tfrac{\eta}{2}(1+K/2)^{1/2}\right] - \tfrac{2}{[\pi(1+K/2)]^{1/2}}\left[1 - \exp\left(-\tfrac{(1+K/2)\eta^2}{4}\right)\right] \\ g(\eta) &= -\tfrac{1}{2}\left(\tfrac{1+K/2}{\pi}\right)^{1/2} \exp\left[-\tfrac{\eta^2}{4}(1+K/2)\right] \end{aligned} \tag{28}$$

The quantity of physical interest in this problem is the local skin friction coefficient C_f, which is defined as, see Cebeci (1979):

$$C_f = \frac{(a/\upsilon) Re^{-1/2} \bar{\tau}_w}{(1/2)\rho u_\infty^2} \tag{29}$$

where $\bar{\tau}_w$ is the wall skin friction given by:

$$\bar{\tau}_w = \left[(\mu + \kappa)\frac{\partial \bar{u}}{\partial \bar{y}} + \kappa \bar{N}\right]_{\bar{y}=0} = [1 + (1-n)K](\mu U_\infty Re^{1/2}/a)\left(\frac{\partial u}{\partial y}\right)_{y=0} \tag{30}$$

Substituting equation (5) into equation (29), we get:

$$C_f = \frac{2[1 + (1-n)K]u_e(x)}{u_\infty} \frac{f''(x,0,t)}{\sqrt{t}} \tag{31}$$

where the reference velocity u_∞ is taken $1/\pi$ and $u_e(x)$ is given by equation (15). At the forward stagnation point, we have $u_e(x) = (1/\pi)\sin(\pi x) \approx x$ and the skin friction coefficient can be expresses as, see Lok *et al.* (2003a):

$$C_f = \frac{[1 + (1-n)K]}{\sqrt{t}} f''(x,0,t) \tag{32}$$

Numerical procedure

Equations (12) and (13) are first written in terms of a first-order system of partial differential equations. In order to eliminate all higher-order derivatives, new dependent variables $u(x, \eta, t)$, $v(x, \eta, t)$ and $p(x, \eta, t)$ are introduced such that:

$$f' = u$$
$$u' = v \tag{33}$$
$$g' = p$$

Here, u and v are new variables that are not related to the flow components in equations (7)-(9). Thus, equations (12) and (13) become:

$$(1+K)v' + \frac{\eta}{2}v + t\frac{\mathrm{d}u_e}{\mathrm{d}x}(1-u^2+fv) + Kp = t\left[\frac{\partial u}{\partial t} + u_e\left(u\frac{\partial u}{\partial x} - v\frac{\partial f}{\partial x}\right)\right] \tag{34}$$

$$\left(1+\frac{K}{2}\right)p' + \frac{\eta}{2}p + \frac{g}{2} + t\frac{\mathrm{d}u_e}{\mathrm{d}x}(fp-ug) = t\left[\frac{\partial g}{\partial t} + u_e\left(u\frac{\partial g}{\partial x} - p\frac{\partial f}{\partial x}\right) + K(2g+v)\right] \tag{35}$$

From equations (20) and (21), the first-order partial differential equations at the stagnation points are as follow:

$$(1+K)v' + \frac{\eta}{2}v + t\lambda(1-u^2+fv) + Kp = t\frac{\partial u}{\partial t} \tag{36}$$

$$\left(1+\frac{K}{2}\right)p' + \frac{\eta}{2}p + \frac{g}{2} + t\lambda(fp-ug) = t\frac{\partial g}{\partial t} + tK(2g+v) \tag{37}$$

Consider the net cube as in Figure 1. The net points are denoted by:

$$\begin{aligned} x_0 &= 0, \quad x_i = x_{i-1} + r_i, \quad i = 1, 2, \ldots, I \\ t_0 &= 0, \quad t_n = t_{n-1} + k_n, \quad n = 1, 2, \ldots, N \\ \eta_0 &= 0, \quad \eta_j = \eta_{j-1} + h_j, \quad j = 1, 2, \ldots, J \end{aligned} \tag{38}$$

where r_i is the Δx-spacing, k_n is the Δt-spacing and h_j is the $\Delta\eta$-spacing.

We approximate the quantities (f, u, v) at points (x_i, t_n, η_j) by the net functions denoted by $f_j^{in}, u_j^{in}, v_j^{in}$. Equations (33) are approximated for the midpoint x_i, t_n, $\eta_{j-1/2}$ using the centered-difference derivatives. Thus, we have:

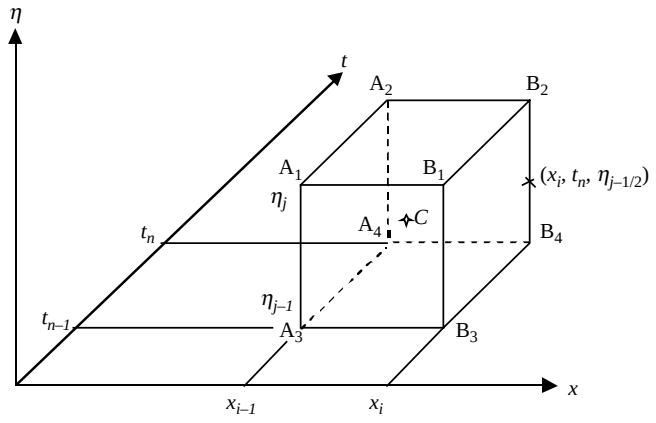

Figure 1.
Net cube for difference approximations

$$\begin{aligned}
\tfrac{1}{h_j}\left(f_j^{i,n}-f_{j-1}^{i,n}\right)&=u_{j-1/2}^{i,n}\\
\tfrac{1}{h_j}\left(u_j^{i,n}-u_{j-1}^{i,n}\right)&=v_{j-1/2}^{i,n}\\
\tfrac{1}{h_j}\left(g_j^{i,n}-g_{j-1}^{i,n}\right)&=p_{j-1/2}^{i,n}
\end{aligned}\tag{39}$$

We next write the finite-difference approximations of equations (34) and (35) at the midpoint $x_{i-1/2}, t_{n-1/2}, \eta_{j-1/2}$ which is an approximation of the function at the center of the three-dimensional box, C. This gives:

$$\begin{aligned}
&\frac{(1+K)}{h_j}\left(v_j^{i,n}-v_{j-1}^{i,n}\right)+\frac{1}{2}\eta_{j-1/2}v_{j-1/2}^{i,n}+t^{n-1/2}\left(\frac{\mathrm{d}u_e}{\mathrm{d}x}\right)^{i-1/2}\left[(fv)_{j-1/2}^{i,n}-(u^2)_{j-1/2}^{i,n}\right]\\
&-Kp_{j-1/2}-2\beta_n u_{j-1/2}^{i,n}-\frac{1}{2}\alpha_i\left[\left(u_{j-1/2}^{i,n}\right)^2+(m_1+m_6)u_{j-1/2}^{i,n}\right.\\
&\left.-v_{j-1/2}^{i,n}f_{j-1/2}^{i,n}-m_3f_{j-1/2}^{i,n}-m_4v_{j-1/2}^{i,n}\right]=m_7
\end{aligned}\tag{40}$$

$$\begin{aligned}
&\frac{(1+K/2)}{h_j}\left(v_j^{i,n}-v_{j-1}^{i,n}\right)+\frac{1}{2}\eta_{j-1/2}p_{j-1/2}^{i,n}+\frac{1}{2}g_{j-1/2}^{i,n}+t^{n-1/2}\left(\frac{\mathrm{d}u_e}{\mathrm{d}x}\right)^{i-1/2}\\
&\times\left[(fp)_{j-1/2}^{i,n}-(ug)_{j-1/2}^{i,n}\right]-2\beta_n g_{j-1/2}^{i,n}-\frac{1}{2}\alpha_i\left(u_{j-1/2}^{i,n}g_{j-1/2}^{i,n}+m_{10}u_{j-1/2}^{i,n}\right.\\
&\left.+m_1g_{j-1/2}^{i,n}-p_{j-1/2}^{i,n}f_{j-1/2}^{i,n}-m_4p_{j-1/2}^{i,n}-m_9f\right)=m_{11}
\end{aligned}\tag{41}$$

where:

$$\begin{aligned}
m_1&=u_{j-1/2}^{234},\\
m_2&=u_{j-1/2}^{i-1,n}-2\bar{u}_{n-1},\\
m_3&=v_{j-1/2}^{234},\\
m_4&=f_{j-1/2}^{i,n-1}-2\bar{f}_{i-1},\\
m_5&=(u^2)_{j-1/2}^{234},\\
m_6&=u_{j-1/2}^{i,n-1}-2\bar{u}_{i-1}\\
m_7&=-\frac{(1+K)}{h_j}\left(v_j^{234}-v_{j-1}^{234}\right)-\frac{1}{2}\eta_{j-1/2}m_3-t^{n-1/2}\left(\frac{\mathrm{d}u_e}{\mathrm{d}x}\right)^{i-1/2}\\
&\quad\times\left[4-m_5+(fv)_{j-1/2}^{234}\right]+Kp_{j-1/2}^{234}+2\beta_n m_2+\frac{1}{2}\alpha_i(m_1m_6m_3m_4)\\
m_8&=g_{j-1/2}^{i-1,n}-2\bar{g}_{n-1},\\
m_9&=p_{j-1/2}^{234},\\
m_{10}&=g_{j-1/2}^{i,n-1}-g_{j-1/2}^{i-1,n}-g_{j-1/2}^{i-1,n-1}
\end{aligned}\tag{42}$$

$$m_{11} = -\frac{(1+K/2)}{h_j}\left(v_j^{234} - v_{j-1}^{234}\right) - \frac{1}{2}\,\eta_{j-1/2}m_9 - \frac{1}{2}g_j^{234} - t^{n-1/2}\left(\frac{\mathrm{d}u_e}{\mathrm{d}x}\right)^{i-1/2}\left[(fp)_{j-1/2}^{234} - (ug)_{j-1/2}^{234}\right] + 2\beta_n m_8 + \frac{1}{2}\,\alpha_i(m_1 m_{10} - m_9 m_4) + t^{n-1/2}K\left(2g_{j-1/2}^{234} + m_3\right)$$

and $()_j^{234} = ()_j^{i-1,n} + ()_j^{i-1,n-1} + ()_j^{i,n-1}$.

The equations at the stagnation points contain only two dependent variables η and t since x is fixed at $x = 0$ for the forward point and $x = 1$ for the rear point. The partial differential equations (36) and (37) are approximated about the midpoint $(x_i,\ t_{n-1/2},\ \eta_{j-1/2})$ of the rectangle $B_1B_2B_3B_4$ which gives:

$$\begin{aligned}&\frac{(1+K)}{h_j}\left(v_j^{i,n} - v_{j-1}^{i,n}\right) + \frac{1}{2}\,\eta_{j-1/2}v_{j-1/2}^{i,n} + t^{n-1/2}\lambda \\ &\quad\times\left[1 - (u^2)_{j-1/2}^{i,n} + (fv)_{j-1/2}^{i,n}\right] + Kp_{j-1/2}^{i,n} - 2\beta_n u_{j-1/2}^{i,n} \\ &= \left\{-\frac{(1+K)}{h_j}(v_j - v_{j-1}) - \frac{1}{2}\,\eta_{j-1/2}v_{j-1/2}\right. \\ &\quad\left.-\hat{\lambda}\left[1 - (u^2)_{j-1/2} + (fv)_{j-1/2}\right] - Kp_{j-1/2} - 2\beta_n u_{j-1/2}\right\}^{n-1}\end{aligned} \tag{43}$$

$$\begin{aligned}&\frac{(1+K/2)}{h_j}\left(p_j^{i,n} - p_{j-1}^{i,n}\right) + \frac{1}{2}\,\eta_{j-1/2}p_{j-1/2}^{i,n} + \frac{1}{2}g_{j-1/2}^{i,n} + t^{n-1/2}\lambda \\ &\quad\times\left[(fp)_{j-1/2}^{i,n} - (ug)_{j-1/2}^{i,n}\right] - 2\beta_n g_{j-1/2}^{i,n} - t^{n-1/2}K\left(2g_{j-1/2}^{i,n} + v_{j-1/2}^{i,n}\right) \\ &= \left\{-\frac{(1+K/2)}{h_j}\left(p_j - p_{j-1}\right) - \frac{1}{2}\,\eta_{j-1/2}p_{j-1/2} - \frac{1}{2}\,g_{j-1/2}\right. \\ &\quad\left.-\hat{\lambda}\left[(fp)_{j-1/2} - (ug)_{j-1/2}\right] - 2\beta_n g_{j-1/2} + t^{n-1/2}K(2g_{j-1/2} + v_{j-1/2})\right\}^{n-1}\end{aligned} \tag{44}$$

where $\hat{\lambda} = t^{n-1/2}\lambda$. Also, the boundary condition (10) become:

$$f_0 = 0, \quad u_0 = 0, \quad g_0 = -nv_0, \quad u_J = 1, \quad g_J = 0 \tag{45}$$

equations (39)-(41), (43) and (44) are nonlinear algebraic equations and the linearization of these equations is carried out using Newton's method. The right hand side of equations (40), (41), (43) and (44) involve only known quantities if we assume that the solution is known at $x = x^{i-1}$ and $t = n^{n-1}y$. Further, we introduce the following iterates:

$$\begin{aligned}&\left\lfloor f_j^{(k)}, u_j^{(k)}, v_j^{(k)}, g_j^{(k)}, p_j^{(k)}\right\rfloor, \quad k = 0, 1, 2, \ldots \\ &f_j^{(k+1)} = f_j^{(k)} + \delta f_j^{(k)}, \quad u_j^{(k+1)} = u_j^{(k)} + \delta u_j^{(k)}, \quad v_j^{(k+1)} = v_j^{(k)} + \delta v_j^{(k)}, \\ &g_j^{(k+1)} = g_j^{(k)} + \delta g_j^{(k)}, \quad p_j^{(k+1)} = p_j^{(k)} + \delta p_j^{(k)}\end{aligned} \tag{46}$$

The above expressions are substituted into the nonlinear system of equations (39)-(41), (43) and (44), and by dropping the terms that are quadratic in $\delta f_j^{(k)}$, $\delta u_j^{(k)}$, $\delta v_j^{(k)}$, $\delta g_j^{(k)}$ and $\delta p_j^{(k)}$, we obtain a linear tridiagonal system of equations.

In a vector-matrix form, it can be written as:

$$\mathbf{A}\delta = \mathbf{r} \tag{47}$$

This tridiagonal matrix can be solved using the block elimination method. These calculations are repeated until the convergence criterion based on the skin friction parameter is satisfied, that is $|\delta f''(x, 0, t) < \varepsilon_1|$ where ε_1 is a small prescribed value. The numerical solution is obtained at some positions x around the cylinder starting from the forward stagnation point $x = x_0 = 0$ and for some values of time t and the micropolar parameter K. All the calculations were done for $n = 0$ (strong concentration) and $n = 1/2$ (weak concentration). We have chosen a step size in t of 0.01, x of 0.025 and η of 0.05, $\eta_\infty = 10$ and the convergence criteria is $\varepsilon_1 = 10^{-6}$. The calculation begins at the initial time $t = 0$ and is progressing until the steady state-flow is reached ($t \to \infty$). Using the initial condition at $t = 0$ as in equation (28), we solve equations (20) and (21) with $\lambda = 1$ (forward stagnation point, $x = 0$) until the convergence criterion is realized. Then, we march to the next x-station, $x = x_1$ up to $x = x_{n-1}$ and equations (12) and (13) are solved using the initial condition at $t = 0$ along with the solution obtained at the previous x-station. Note that the convergence criteria is checked at each x-station. For the solution at the rear stagnation point, x_n, the same procedure is applied and equations (20) and (21) are solved by choosing $\lambda = -1$. After the converged solutions at all x-stations are obtained, we then march to the next t-station. The solutions at the current t-station can be found using the converged solutions at the previous t-station and the same procedure as explained above is applied by marching from x_0 up to x_n.

Results and discussion

Values of the skin friction coefficient C_f at the forward stagnation point ($x = 0$), given by equation (32), are given in Table I for some values of time t and material parameter K when $n = 0$ (strong concentration). The values obtained by Cebeci (1979) for $K = 0$ (Newtonian fluid) and Lok *et al.* (2003c) for $K = 0$, 0.5, 1, 1.5, 2 and 3 are also included in this table. It is seen that for a fixed value of t, C_f increases with the increase:

$$F''_w = \frac{1}{u_e}\left(\frac{\partial u}{\partial y}\right)_w \tag{48}$$

of K and it decreases to its steady-state value when t increases and K is fixed. Further, Table II shows the values of the wall skin friction, F''_w, given by equation (48), for some values of t and K when $n = 1/2$ (weak concentration). Again, the values reported by Cebeci (1979) for $K = 0$ (Newtonian fluid) and Lok *et al.* (2003b) for $K = 0$, 0.5, 1, 1.5, 2 and 3 are included in this table. It is observed that for all values of K considered, the numerical values of F''_w are in excellent agreement with those reported by Cebeci (1979) and Lok *et al.* (2003b). The numerical values indicate that increasing K results in a decrease in the values of F''_w when t is held fixed. This is because as K increases, the thickness of the velocity boundary becomes larger and thus it gives rise to a reduction of F''_w. It is also seen that the numerical solution approaches monotonically, for all values of K considered, the steady-state value of F''_w. However, the steady-state values of F''_w are lower for the greater values of K. Results of Table II are also shown in Figure 2, which displays the variation of F''_w with t at the forward stagnation point ($x = 0$) for some values of K when $n = 1/2$. The values reported by Cebeci (1979) for

T	$K = 0$	$K = 0.5$	$K = 1.0$	$K = 1.5$	$K = 2.0$	$K = 3.0$
0.01	5.722594	7.005407	8.081295	9.024262	9.872381	11.366978
	5.722541	7.005393	8.081298	9.024277	9.872415	11.367033
0.04	2.980922	3.6446073	4.193333	4.667595	5.088453	5.816257
	2.980900	3.644602	4.193344	4.667630	5.088528	5.816459
0.09	2.118524	2.585566	2.964030	3.285159	3.565468	4.040375
	2.118525	2.585574	2.964048	3.285196	3.565534	4.040536
0.16	1.724063	2.099876	2.397875	2.646304	2.860266	3.218375
	1.724086	2.099899	2.397902	2.646343	2.860326	3.218494
0.25	1.514670	1.841165	2.095033	2.303997	2.482818	2.782084
	1.514717	1.841204	2.095072	2.304041	2.482873	2.782167
0.36	1.395589	1.693421	1.921517	2.108099	2.267849	2.537340
	1.395665	1.693483	1.921572	2.108153	2.267904	2.537399
0.49	1.325873	1.606516	1.819292	1.993209	2.142784	2.397505
	1.325986	1.606606	1.819369	1.993277	2.142847	2.397559
0.64	1.284858	1.555125	1.758892	1.925844	2.070179	2.317669
	1.285016	1.555251	1.758997	1.925934	2.070259	2.317732
0.81	1.261001	1.525080	1.723710	1.887000	2.028739	2.272650
	1.261216	1.525250	1.723851	1.887120	2.028845	2.272734
1	1.247448	1.507930	1.703764	1.865228	2.005720	2.247802
	1.247727	1.508152	1.703948	1.865386	2.005860	2.247917
1.21	1.239991	1.498462	1.692863	1.853469	1.993371	2.234487
	1.240346	1.498744	1.693098	1.853672	1.993552	2.234639
1.44	1.236042	1.493442	1.687160	1.847385	1.987008	2.227611
	1.236482	1.493793	1.687454	1.847640	1.987237	2.227804
1.69	1.234031	1.490897	1.684317	1.844381	1.983873	2.224207
	1.234565	1.491323	1.684675	1.844694	1.984154	2.224446
1.96	1.233040	1.489659	1.682964	1.842965	1.982396	2.222598
	1.233677	1.490169	1.683393	1.843341	1.982734	2.222886
2.25	1.232556	1.489075	1.682343	1.842322	1.981726	2.221869
	1.233304	1.489674	1.682849	1.842765	1.982126	2.222211
2.56	1.232309	1.488795	1.682059	1.842033	1.981428	2.221554
	1.233176	1.489490	1.682646	1.842549	1.981893	2.221946
2.89	1.232163	1.488648	1.681919	1.841895	1.981290	2.221404
	1.233157	1.489446	1.682593	1.842488	1.981824	2.221861
Steady	*1.23259*	*1.488986*	*1.682170*	*1.842086*	*1.981438*	*2.221496*
	1.232627					

Sources: Cebeci (1979) and Lok *et al.* (2003c)

Table I.
Values of the skin friction coefficient C_f as a function of t at the forward stagnation point ($x = 0$) for various values of K when $n = 0$ (strong concentration)

a Newtonian fluid ($K = 0$) are also included in this figure. We notice again that for a Newtonian fluid ($K = 0$) an excellent agreement exists between the present results and those reported by Cebeci (1979). This figure also shows that at t increases, F''_w tends monotonically to the steady-state values.

The variation of the skin friction coefficient C_f with t near the rear stagnation point ($x = 1$) of the cylinder is shown in Figures 3 and 4 for $n = 0$ and 1/2, respectively. The results obtained by Lok *et al.* (2003b) have also been included in Figure 4, which show a very good agreement with the present results. The point of the boundary layer separation $x = x_s$ is found at $t = t_s = 0.6438, 0.6096, 0.5803$ and 0.5644 for $n = 0$ with $K = 0, 1, 2$ and 3, respectively. Also, $t = t_s = 0.6438$ for $n = 1/2$ and all values of K considered. We notice that the values of C_f for the micropolar fluid ($K \neq 0$) are

t	$K = 0$	$K = 0.5$	$K = 1.0$	$K = 1.5$	$K = 2.0$	$K = 3.0$
0.01	5.722594 5.722541	5.118331	4.67232	4.325689	4.046285	3.61909
0.04	2.980922 2.980900	2.66616	2.433831	2.25327	2.107727	1.885197
0.09	2.118524 2.118525	1.894824	1.729711	1.601388	1.497951	1.339795
0.16	1.724063 1.724086	1.542016	1.407648	1.303218	1.219041	1.090331
0.25	1.51467 1.514717	1.354735	1.236687	1.144942	1.070989	0.957911
0.36	1.395589 1.395665	1.248229	1.139464	1.054932	0.986794	0.882606
0.49	1.325873 1.325986	1.185878	1.082548	1.00224	0.940242	0.838525
0.64	1.284858 1.285016	1.149196	1.049065	0.971243	0.908513	0.812595
0.81	1.261001 1.261216	1.127863	1.029594	0.953219	0.891655	0.797519
1	1.247448 1.247727	1.115745	1.018534	0.942984	0.882083	0.788961
1.21	1.239991 1.240346	1.109081	1.012455	0.93736	0.876825	0.784262
1.44	1.236042 1.236482	1.105661	1.009241	0.934388	0.874048	0.781782
1.69	1.234031 1.234565	1.103812	1.007611	0.932884	0.87276	0.78053
1.96	1.23304 1.233677	1.102885	1.006815	0.932152	0.871962	0.779925
2.25	1.232556 1.233304	1.102461	1.006435	0.931804	0.871641	0.779643
2.56	1.232309 1.233176	1.102249	1.006249	0.931637	0.871489	0.779511
2.89	1.232163 1.233157	1.102128	1.006147	0.931548	0.87141	0.779446
Steady	*1.23259* *1.232627*	*1.102488*	*1.006425*	*0.931766*	*0.871585*	*0.779567*

Table II.
Values of the skin friction coefficient F''_w as a function of t at the forward stagnation point ($x = 0$) for various values of K when $n = 1/2$ (weak concentration)

Sources: Cebeci (1979) and Lok *et al.* (2003b)

higher compared to that for the Newtonian fluid ($K = 0$). From these results it can be, therefore, concluded that the developed code for the present 3D unsteady boundary layer can be used with great confidence to study the problem discussed in this paper.

Figures 5-12 show the velocity profiles f' and microrotation profiles $-g$ at both the forward stagnation point ($x = 0$) and rear stagnation point ($x = 1$) for different values of time t when $K = 0$ (Newtonian fluid) and $K = 2$ for $n = 0$ and $n = 1/2$, respectively. The results for unsteady flows reported by Lok *et al.* (2003c) have also been included in Figure 5, while the results for the steady-state case are included in Figures 5 and 6 show an excellent agreement with the present results. It is seen that as the time progresses, the velocity profiles at the forward stagnation point approach the

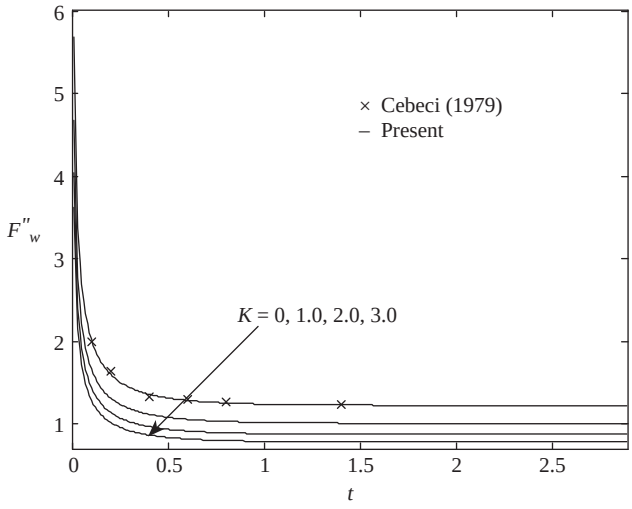

Figure 2.
Variation of the wall skin friction parameter F''_w with t at $x = 0$ (forward stagnation point) for various values of K when $n = 1/2$ (weak concentration)

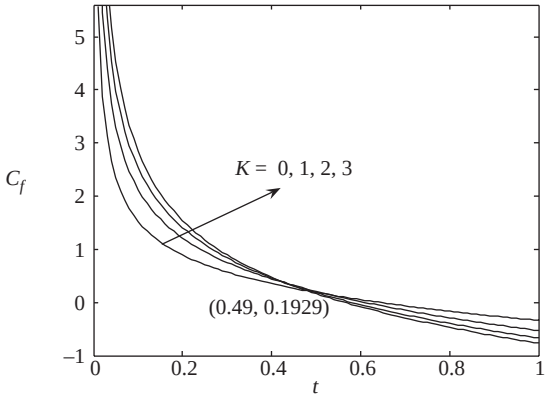

Figure 3.
The skin friction coefficient at $x = 1$ (rear stagnation point) for various values of K when $n = 0$ (strong concentration)

steady-state solution. The results obtained by Cebeci (1979) for a Newtonian fluid ($K = 0$) when $t = 0.5$ are also included in Figure 7. The velocity profiles at the rear stagnation point ($x = 1$) are shown in Figure 8 for $n = 0$ and $n = 1/2$ when $K = 2$. We can see that these velocity profiles develop rapidly from rest and as K increases the boundary layer thickness increases considerably. On the other hand, we notice that at the forward stagnation point, the microrotation profiles $-g$ start at $-g(x = 0, 0, t) = 0$, for $n = 0$, while for $n = 1/2$ these profiles start at $-g(x = 0, 0, t) = (1/2)\ f''(x = 0, 0, t)$, see Figures 9 and 10. For $n = 0$, $-g$ profiles reach at both forward and rear stagnation points, maximum values inside the boundary layer and then decrease to zero, as we can see in Figures 9 and 11. On the other hand, Figure 12 shows the profiles of $-g$ at the rear stagnation point for $n = 1/2$ and $K = 2$. One can see that $-g$ profiles reach the maximum values at the wall ($\eta = 0$) when t is small. For larger values of t, the maximum values are inside boundary layer.

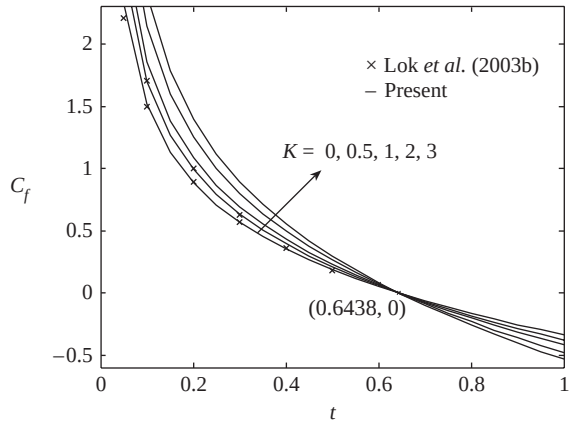

Figure 4.
The skin friction coefficient at $x = 1$ (rear stagnation point) for various values of K when $n = 1/2$ (weak concentration)

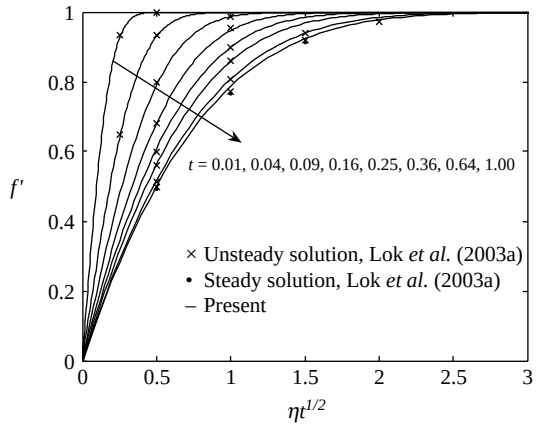

Figure 5.
The velocity profiles at $x = 0$ (forward stagnation point) for various values of t when $K = 0$ (Newtonian fluid)

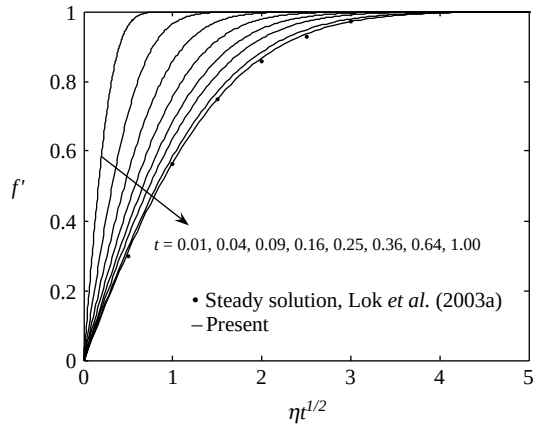

Figure 6.
The velocity profiles at $x = 0$ (forward stagnation point) for various values of t when $K = 2$ and $n = 0$ (strong concentration)

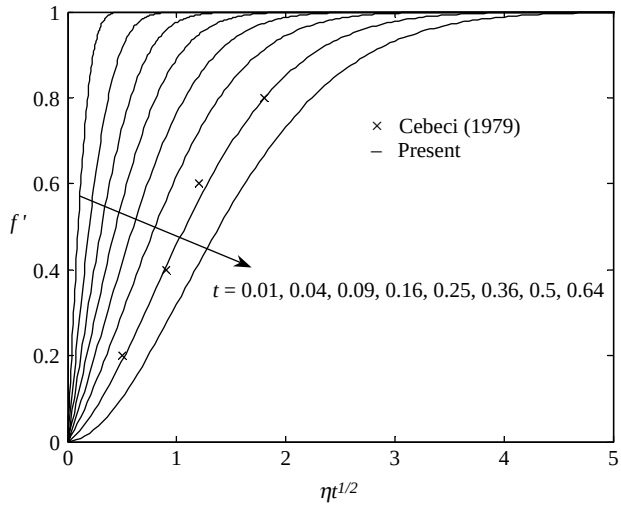

Figure 7.
The velocity profile at $x = 1$ (rear stagnation point) for values of t when $K = 0$ (Newtonian fluid)

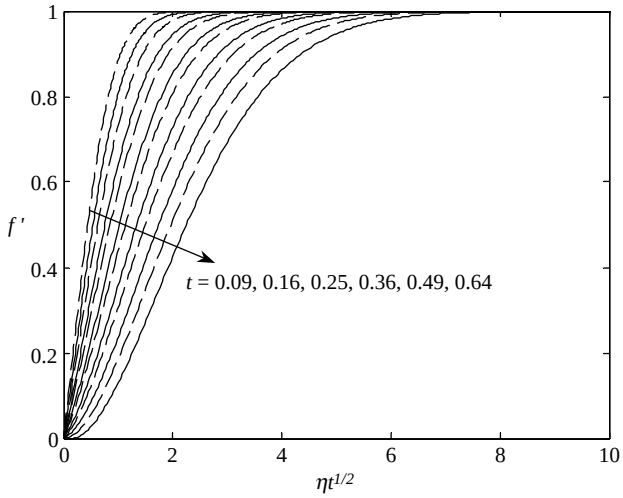

Figure 8.
The velocity profiles at $x = 1$ (rear stagnation point) when $K = 2$: $-n = 0$ (strong concentration), $- -$ $n = 1/2$ (weak concentration)

Figures 13 and 14 show the variation of the microrotation profiles $-g$ with $\eta t_{1/2}$ at $x = 0.5$ when $K = 2$ for $n = 0$ and $n = 1/2$. We can see that the microrotation profiles $-g$ increase with the increase of t. On the other hand, we notice that for $n = 0$ the microrotation profiles start at $-g(x = 0.5, 0, t) = 0$, while for $n = 1/2$ these profiles start at $-g(x = 0.5, 0, t) = (1/2)f''(x = 0.5, 0, t)$, see Figures 13 and 14. For $n = 0$ these profiles reach maximum values inside the boundary layer and then decrease to zero. However, the maximum values of $-g$ profiles are reached at the wall ($\eta = 0$) for $n = 1/2$, see Figure 14.

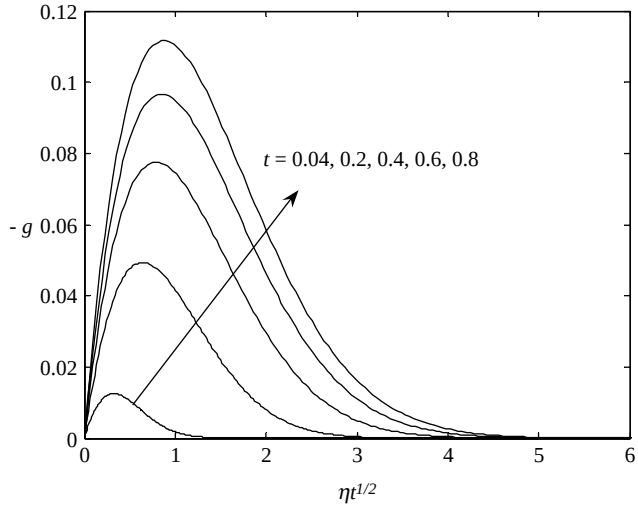

Figure 9.
Microrotation profiles at $x = 0$ (forward stagnation point) for various values of t when $K = 2$ and $n = 0$ (strong concentration)

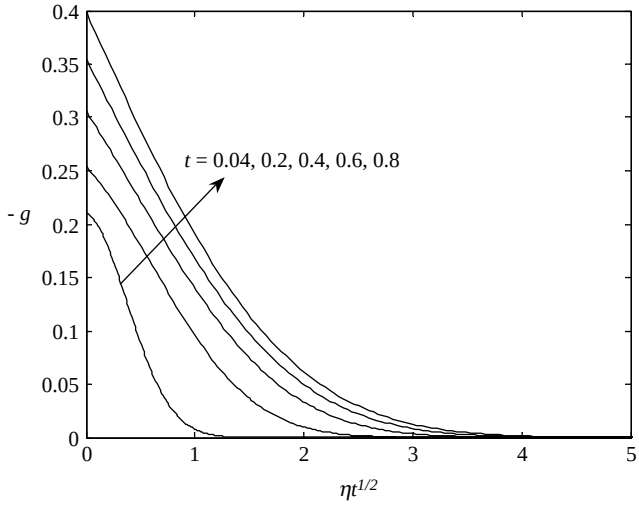

Figure 10.
Microrotation profiles at $x = 0$ (forward stagnation point) for various values of t when $K = 2$ and $n = 1/2$ (weak concentration)

Variation of the skin friction coefficient C_f, given by equation (31), with the coordinate x measured along the surface of the cylinder is shown in Figures 15-17 for $K = 0$ (Newtonian fluid) and $K = 2$ when $n = 0$ and $n = 1/2$. The results obtained by Bar-Lev and Yang (1975), and Cebeci (1979) for $K = 0$ are also included in Figure 15. We can see that a very good agreement between the present results and those obtained by Bar-Lev and Yang (1975), and Cebeci (1979) exist. Further, it is seen from Figures 15-17 that as the fluid moves from the forward stagnation point ($x = 0$) to the rear stagnation point ($x = 1$), the value of C_f increases from zero to the maximum value and it decreases back

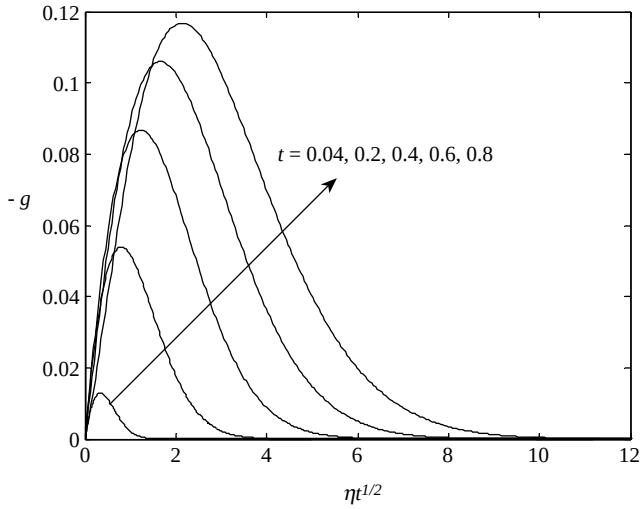

Figure 11.
Microrotation profiles $x = 1$ (rear stagnation point) for various values of t when $K = 2$ and $n = 0$ (strong concentration)

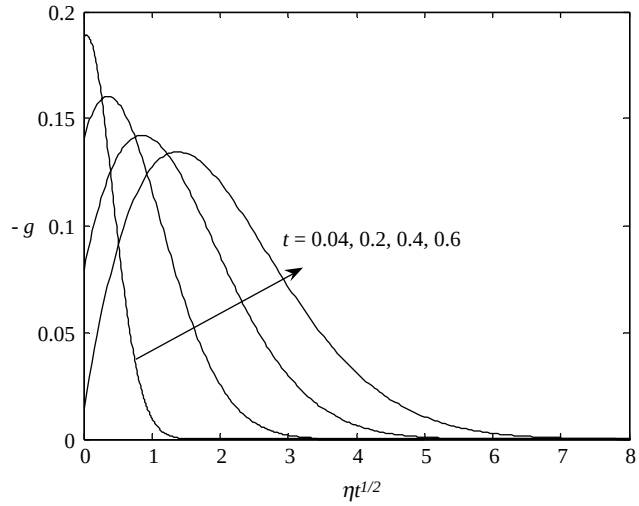

Figure 12.
Microrotation profiles $x = 1$ (rear stagnation point) for various values of t when $K = 2$ and $n = 1/2$ (weak concentration)

to zero at the rear stagnation point. This maximum value is higher for smaller values of t. We also observe from the present study that this maximum value is higher for the micropolar fluid ($K \neq 0$) than that for the Newtonian fluid ($K = 0$).

Values of the separation time T_s around the cylinder ($\theta = x/a$) are shown in Table III for different values of K. In order to compare the present results for $K = 0$ (Newtonian fluid) with those of Bar-Lev and Yang (1975), Katagiri (1976) and Cebeci (1979), we have taken the time $t = 2T$. The results are again found in excellent agreement. We then notice that for $K = 0$ (Newtonian fluid), the point of separation θ_s first appears

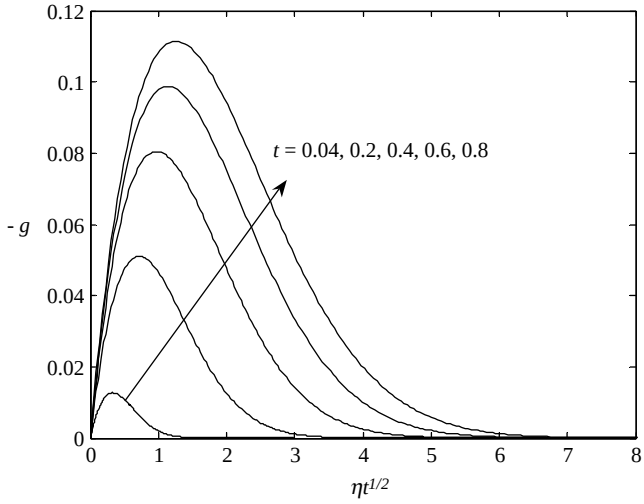

Figure 13.
Microrotation profiles at $x = 0.5$ for various values of t when $K = 2$ and $n = 0$ (strong concentration)

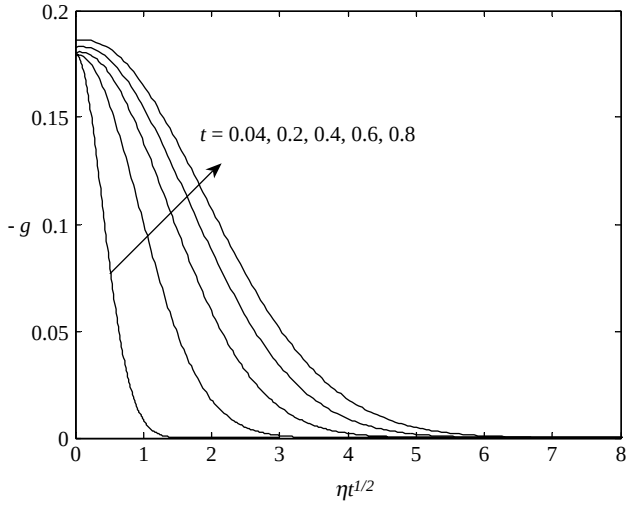

Figure 14.
Microrotation profiles at $x = 0.5$ for various values of t when $K = 2$ and $n = 1/2$ (weak concentration)

at the rear stagnation point ($x = 1$) when $T_s = 0.3219$, which then spreads to other points along the cylinder surface as time T increases. The separation occurs at the lower value of time as the value of K increases. Finally, Figure 18 shows the variation of the position θ_s of the boundary layer separation along the cylinder surface with T_s for $K = 0$ (Newtonian fluid) and $K = 2$ when $n = 0$. The results of Cebeci (1979) for $K = 0$ are also included in this figure. It is seen again that the present results are in very good agreement with those obtained by Cebeci (1979).

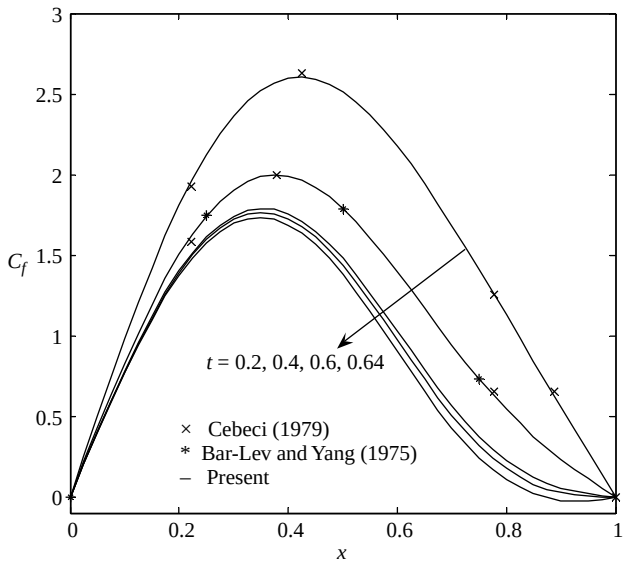

Figure 15.
Variation with x of the skin friction coefficient around the cylinder when $K = 0$ (Newtonian fluid)

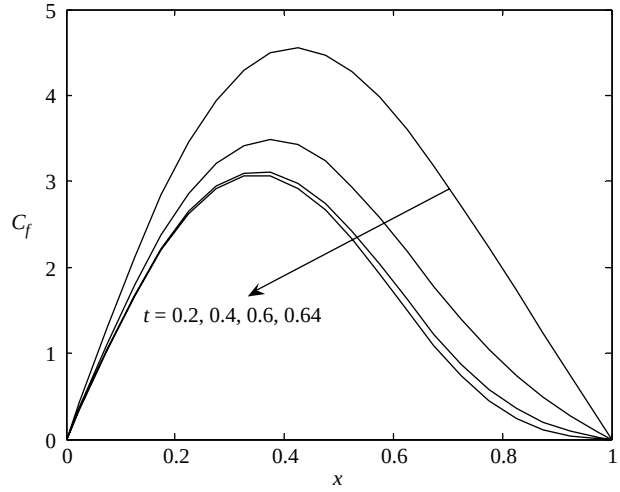

Figure 16.
Variation with x of the skin friction coefficient around the cylinder when $K = 2$ and $n = 0$ (strong concentration)

Conclusions

The 3D Keller-box method is applied to the problem of unsteady boundary layer flow past an impulsively started circular cylinder in a micropolar fluid. Numerical solutions are presented for the time up to the point of separation and good agreement with published results has been established.

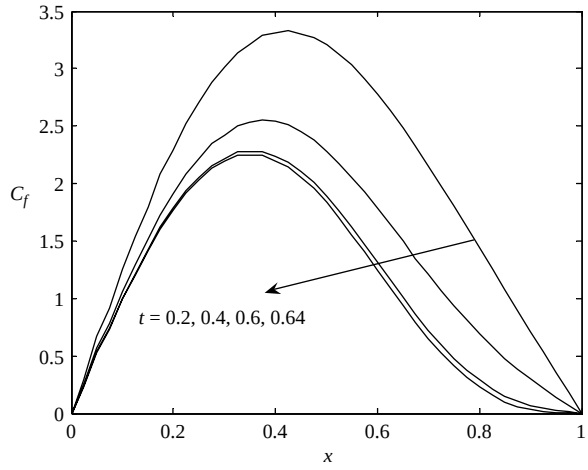

Figure 17.
Variation with x of the skin friction coefficient around the cylinder when $K = 2$ and $n = 1/2$ (weak concentration)

Author	$\theta = 180$	166	146	138	124	110
$K = 0$ (Newtonian fluid)						
Cebeci (1979)	$T_s = 0.320$	0.330	0.390	0.436	0.596	1.10
Bar-Lev and Yang (1975)	$= 0.322$	0.330	0.389	0.438	0.602	1.089
Katagiri (1976)	$= 0.3214$					1.0640
Present results for $n = 0$						
$K = 0$	$T_s = 0.3219$	0.3327	0.3918	0.4418	0.598	1.0816
$K = 0.5$	$= 0.3149$	0.3255	0.3833	0.4283	0.5822	1.0389
$K = 1.0$	$= 0.3048$	0.3138	0.3691	0.4123	0.5572	0.9813
$K = 1.5$	$= 0.2965$	0.3020	0.3540	0.3944	0.5341	0.9294
$K = 2.0$	$= 0.2855$	0.2894	0.3428	0.3771	0.5005	0.8795

Table III.
Values of the separation time T_s around the cylinder ($\theta = x/a$) for different values of the material parameter K

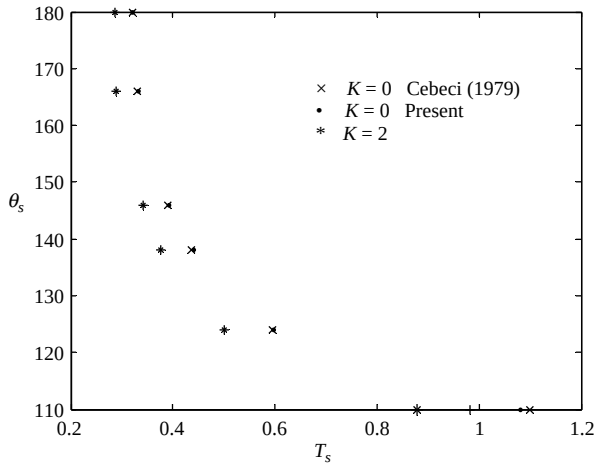

Figure 18.
Variation of the separation point θ_s with T_s for $K = 0$ (Newtonian fluid), $K = 1$ and 2 when $n = 0$ (strong concentration)

References

Ahmadi, G. (1976), "Self-similar solution of incompressible micropolar boundary layer flow over a semi-infinite plate", *Int. J. Engng. Sci.*, Vol. 14, pp. 639-46.

Ariman, T., Turk, M.A. and Sylvester, N.D. (1973), "Microcontinuum fluid mechanics – a review", *Int. J. Engng. Sci.*, Vol. 11, pp. 905-30.

Ariman, T., Turk, M.A. and Sylvester, N.D. (1974), "Application of microcontinuum fluid mechanics", *Int. J. Engng. Sci.*, Vol. 12, pp. 273-93.

Bar-Lev, M. and Yang, H.T. (1975), "Initial flow field over an impulsively started circular cylinder", *J. Fluid Mech.*, Vol. 72, pp. 625-47.

Cebeci, T. (1979), "The laminar boundary layer on a circular cylinder started impulsively from rest", *J. Comp. Phys.*, Vol. 31, pp. 153-72.

Cebeci, T. (1986), "Unsteady boundary layer with an intelligent numerical scheme", *J. Fluid Mech.*, Vol. 163, pp. 129-40.

Collins, W.M. and Dennis, S.C.R. (1973a), "The initial flow past an impulsively started circular cylinder", *Q.J. Mech. Appl. Math.*, Vol. 26, pp. 53-75.

Collins, W.M. and Dennis, S.C.R. (1973b), "Flow past an impulsively started circular cylinder", *J. Fluid Mech.*, Vol. 60, pp. 105-27.

Eringen, A.C. (1966), "Theory of micropolar fluids", *J. Math. Mech.*, Vol. 16, pp. 1-18.

Eringen, A.C. (1972), "Theory of thermomicrofluids", *J. Math. Anal. Appl.*, Vol. 38, pp. 480-96.

Eringen, A.C. (2001), *Microcontinuum Field Theories. II: Fluent Media*, Springer, New York, NY.

Gorla, R.S.R. (1988), "Combined forced and free convection in micropolar boundary layer flow on a vertical flat plate", *Int. J. Engng. Sci.*, Vol. 26, pp. 385-91.

Guram, G.S. and Smith, C. (1980), "Stagnation flows of micropolar fluids with strong and weak interactions", *Comp. Math. Appl.*, Vol. 6, pp. 213-33.

Hassanien, I.A., El-Hawary, H.M. and Salama, A.A. (1996), "Chebyshev solution of axisymmetric stagnation flow on a cylinder", *Energy Convers. Mgmt.*, Vol. 37, pp. 67-76.

Ingham, D.B. (1984), "Unsteady separation", *J. Comput. Phys.*, Vol. 53, pp. 90-9.

Jena, S.K. and Mathur, M.N. (1981), "Similarity solutions for laminar free convection flow of a thermomicropolar fluid past a nonisothermal flat plate", *Int. J. Engng. Sci.*, Vol. 19, pp. 1431-9.

Kamal, M.A. and Siddiqui, A.Z.A. (2004), "Micropolar fluid flow due to rotating and oscillating circular cylinder: 6th order numerical study", *J. Appl. Math. Mech. (ZAMM)*, Vol. 84, pp. 96-113.

Katagiri, M. (1976), "Unsteady boundary layer flows past an impulsively started circular cylinder", *J. Phys. Soc. Japan*, Vol. 40, pp. 1171-7.

Kline, K.A. (1977), "A spin-vorticity relation for unidirectional plane flows of micropolar fluids", *Int. J. Engng. Sci.*, Vol. 15, pp. 131-4.

Lok, Y.Y., Amin, N. and Pop, I. (2003a), "Unsteady boundary layer flow of a micropolar fluid near the rear stagnation point of a plane surface", *Int. J. Thermal Sci.*, Vol. 42, pp. 995-1001.

Lok, Y.Y., Amin, N. and Pop, I. (2003b), "Steady two-dimensional asymmetric stagnation point flow of a micropolar fluid", *J. Appl. Math. Mech. (ZAMM)*, Vol. 83, pp. 594-602.

Lok, Y.Y., Phang, P., Amin, N. and Pop, I. (2003c), "Unsteady flow of a micropolar fluid near the forward stagnation points of a plane surface", *Int. J. Engng. Sci.*, Vol. 41, pp. 173-86.

Łukaszewicz, G. (1999), *Micropolar Fluids: Theory and Application*, Birkhäuser, Basel.

McCroskey, W.J. (1977), "Some current research in unsteady fluid dynamics – the 1976 Freeman scholar lecture", *ASME J. Fluids Engng.*, Vol. 99, pp. 8-38.

Nam, S. (1990), "Higher-order boundary-layer solution for unsteady motion of a circular cylinder", *J. Flui Mech.*, Vol. 214, pp. 89-110.

Nath, G. (1976), "Nonsimilar incompressible laminar boundary-layer flows in micropolar Fluids", *Rheologica Acta.*, Vol. 15, pp. 209-14.

Patel, V.A. (1976), "Time-dependent solutions of the viscous incompressible flow past a circular cylinder by the method of series truncation", *Comp. & Fluids*, Vol. 4, pp. 13-27.

Prandtl, L. (1905), "Über Flüssigkeitsbewegung bei sehr kleiner Reibung", *Verhandlungen des Dritten Internationalen Mathematiker-Kongresses*, Leipzig, S., Heidelberg, pp. 484-91.

Rayleigh, L, (1911), "On the motion of solid bodies through viscous fluid", *Phil. Mag.*, Vol. 21, pp. 697-711.

Rees, D.A.S. and Bassom, A.P. (1996), "The Blasius boundary-layer flow of a micropolar fluid", *Int. J. Engng. Sci.*, Vol. 34, pp. 113-24.

Riley, N. (1975), "Unsteady laminar boundary layers", *SIAM Review*, Vol. 17, pp. 274-97.

Riley, N. (1990), "Unsteady viscous flows", *Sci. Progress*, Vol. 74, pp. 361-77.

Shu, C., Khoo, B.C., Chew, Y.T. and Yeo, K.S. (1996), "Numerical studies of unsteady boundary layer flows past an impulsively started circular cylinder by GDQ and GIQ approaches", *Comp. Meth. Appl. Mech.& Engng.*, Vol. 135, pp. 229-41.

Stokes, G.G. (1851), "On the effect of the internal friction of fluids on the motion of pendulums", *Transactions of the Cambridge Philosophical Society*, Vol. 9, pp. 8-106.

Tani, I. (1977), "History of boundary-layer theory", *Ann. Rev. Fluid Mech.*, Vol. 9, pp. 87-111.

Telionis, D.P. (1979), "Review – unsteady boundary layers, separated and attached", *ASME J. Fluids Engng.*, Vol. 101, pp. 29-43.

Telionis, D.P. (1981), *Unsteady Viscous Flows*, Springer, Berlin.

Wang, C-Y. (1967), "The flow past a circular cylinder which is started impulsively from rest", *J. Math. Phys.*, Vol. 46, pp. 195-202.

Wang, C-Y. (1968), "A note on the drag of an impulsively started circular cylinder", *J. Math. Phys.*, Vol. 47, pp. 451-5.

Yücel, A. (1989), "Mixed convection in micropolar fluid flow over a horizontal plate with surface mass transfer", *Int. J. Engng. Sci.*, Vol. 27, pp. 1593-602.

Corresponding author
Ioan Pop can be contacted at: pop.ioan@yahoo.co.uk